The Effective Width in Composite Steel Concrete Beams at Ultimate Loads

Dr. Mohannad Husain Mohsen
Instructor
College of Engineering-University of Baghdad
email:mhnd7@yahoo.com

Salam Naseer Mohammed*
M.Sc. student
College of Engineering-University of Baghdad
email:salamnaseer@yahoo.com

ABSTRACT

A composite section is made up of a concrete slab attached to a steel beam by means of shear connectors. Under positive and negative bending moment, part of the slab will act as a flange of the beam, resisting the longitudinal compression or tension force. When the spacing between girders becomes large, it is evident that the simple beam theory does not strictly apply because the longitudinal stress in the flange will vary with distance from the girder web, the flange being more highly stressed over the web than in the extremities. This phenomenon is termed "shear lag".

In this paper, a nonlinear three-dimensional finite element analysis is employed to evaluate and determine the actual effective slab width of the composite steel-concrete beams by using the Analysis System computer program (ANSYS 11.0).

The of elements were used (SOLID65, LINK8, SHELL143, COMBIN39, TARGE170 and CONTA174) to model the concrete slab, the steel reinforcing bars, the steel girder, the shear connectors (including uplift and dowel action), and the interface between top flange of the steel girder and concrete slab, respectively.

Comparisons with experimental tests have been performed to validate the finite element analysis results. In general, excellent agreement between the finite element solution and the experimental results has been obtained. The maximum difference in ultimate load is about (2.9%).

Finally, parametric studies have been carried out to investigate the effect of some important parameters; these parameters include the degree of interaction, slab thickness, slab width, concrete compressive strength (f'_c), distribution of shear connectors, reinforcement of slab, type of loading, and boundary conditions. The effect of changing these parameters causes variety in the effective slab width and the maximum stress reaches 40.7% and 28.5%, respectively.

Keywords: shear lag, effective width, composite beams, partial interaction, nonlinear analysis

العرض الفعال في العتبات المركبة من الفولاذ والخرسانة عند الحمل الاقصى

د. مهند حسين محسن
مدرس
كلية الهندسة – جامعة بغداد

سلام نصير محمد
ماجستير
كلية الهندسة – جامعة بغداد

الخلاصة

ان المقطع المركب يتكون من شفة خرسانية مربوطة بعارضة فولاذية بواسطة روابط القص. تحت عزم الإنحناء الموجب والسالب جزء من البلاطة يعمل كجزء من العتبة لمقاومة الشد أو الانضغاط الطولي. عندما تصبح المسافة بين العوارض الفولاذية كبيرة،فان نظرية العتبة البسيطة لا تنطبق بدقة لأن الإجهاد الطولي في الحافات سيتفاوت حسب المسافة من وترة العارضة. حيث ان مناطق الشفة القريبة من الوترة تكون تحت إجهادات أكبر من الحافة البارزة البعيدة،فان هذه الظاهرة تسمى "تخلف القص".

اعتمدت هذه الرسالة تحليل لاخطي ثلاثي الأبعاد ، بإستخدام طريقة العناصر المحددة ، لتقييم وتحديد عرض الشفة الفعال للعتبة الفولاذية الخرسانية المركبة بأستخدام برنامج الحاسوب (ANSYS 11.0).

أستخدمت عناصر محددة مختلفة (SOLID65, LINK8, SHELL143, COMBIN39, TARGE170 CONTA174) لتمثيل البلاطة الخرسانية وحديد التسليح والعارضة الفولاذية وروابط القص (متضمناً الانفصال والانزلاق) والمنطقة البينية.

للتحقق من صحة التمثيل تم إجراء مقارنة مع فحوصات عملية لأعتاب مركبة. وقد كانت النتائج متوافقة بشكل ممتاز. وأكبر نسبة فرق في التحمل الأقصى كانت 2.9%.

أخيراً ،لقد أجريت عدة دراسات لتحري تأثير بعض المتغيرات المهمة. زمن تلك المتغيرات تأثيردرجة الارتباط وتأثير سمك البلاطة وتاثير عرض الشفة وتأثير مقاومة الانضغاط للخرسانة وتأثير توزيع رابطات القص وتأثير كمية حديد التسليح في البلاطة وتأثير نوع الإسناد والتحميل.ان تأثير التغاير في هذه المتغيرات قد سبب إختلاف عرض الشفة الفعال و أعظم إجهاد فيها بمقدار 40.7% و 28.5% على التوالي.

1. INTRODUCTION

Composite steel-concrete structures are used widely in bridge and building construction. A composite member is formed when a steel component, such as an I-section beam, is attached to a concrete component, such as a floor slab or bridge deck. The fact that each material is used to take advantage of its best attributes makes composite steel-concrete construction very efficient and economical. However, the real attraction of composite construction is based on having an efficient connection of the steel to the concrete, and it is this connection that allows a transfer of forces and given composite member unique behavior [Oehlers and Bradford, 1999]. Although the word composite may refer to all kinds of different materials connected together, in this study the term composite construction means steel girder attached to a reinforced concrete slab by means of mechanical connectors, **Fig. 1**. The functions of these connectors are to transfer horizontal and normal forces between the two components, thus sustaining the composite action.

2. SHEAR LAG

The thin slab of cellular and beam and slab decks can be thought of as flanges of I- or T-beams. When such I- or T-beam are flexed, the compression/tension force in each flange near mid span is injected into the flange by longitudinal edge shear forces. Under the action of the axial compression and eccentric edge shear flows, the flange distorts as shown in **Fig. 2** and does not compress as assumed in simple beam theory with plane sections remaining plane. The amount of distortion depends on both the shape of the flange in plane and on the distribution of shear flow along its edge. As is shown in **Fig. 2**, a narrow flange distorts little and its behavior approximates to that assumed in simple beam theory. In contrast, the wide flanges distort seriously because the compression induced by the edge shears does not flow very far from the loaded edge, and much of each wide flange is ineffective. The decrease in flange compression away from the loaded edge due to shear distortion is called (shear lag) ,**Hamply, 1976**.

Shear lag has long been of interest to researches. **Adekola, 1974,** formulated and solved constitutive equations which relate partial interaction with shear lag by series solutions for deflections and in-plane stress in the slab to satisfy all the known boundary conditions. **Foutch** and **Chang, 1982,** investigated the effects of shear lag and shear deformation on the static and dynamic response of tapered thin-walled box beams. **Dezi et al. 2001** proposed a model for analyzing the shear-lag effect in composite beams with flexible shear connection. **Sun and Bursi, 2005,** proposed displacement-based and two-filed mixed beam elements for the linear analysis of steel–concrete composite beams with shear lag and deformable shear connection. **Chiewanichakorn et al. 2004,** introduced a three-dimensional non-linear finite element analysis to evaluate and determine the actual effective slab width of steel-composite bridge girders. **Aref et al. 2007,** investigated the behavior of steel–concrete composite girders mainly under applied negative moment to develop and apply an appropriate effective slab width definition. **Zhou 2011,** presented a new F.E.M. to be proposed for the analysis of shear lag effect in box girders under prestressing.

3. EFFECTIVE SLAB WIDTH

Effective width definition has traditionally been based on the distribution of longitudinal stress across the slab width. This definition takes effective width as the equivalent width of slab having a constant stress distribution across it and sustaining a force that is equal to interaction axial force in each of the elements of

the composite system. The magnitude of the constant stress is taken as the peak longitudinal stress in the slab at the slab-beam junction [Adekola, 1974[b]], as shown in **Fig. 3.**

Many researchers, **Mackey, 1961**; **Adekola, 1968**; **Ansourian, 1975**; **Heins, 1976**; **Elkelish, 1986**; and **Oehlers** and **Bradford, 1999**, used Eq. (1) to calculate the effective slab width in composite beams.

$$2\bar{b}=\frac{2\int_0^b \sigma_y\, dx}{(\sigma_y)_{max}} \tag{1}$$

Where ($2\bar{b}$) is the effective width of the concrete slab, (b) is a half slab width, (σ_y) represent the normal stress in the longitudinal direction in the slab at top surface, and $(\sigma_y)_{max}$ is the maximum normal stress between $0 \le x \le b$ **Fig. 4.**

The numerator of the Eq. (1) was calculated by an approximate method using trapezoidal rule; these calculations were done by MATLAB (R2010a) computer program.

3.1 Effective Width in Codes of Practice

The effective width concept has been widely recognized and implemented into different codes of practice around the world. The formulas used by various codes are shown in **Table 1**.

4. BRIDGE DESIGN SPECIFICATIONS

4.1 British Specification [BSI 1979, BSI 1982]

In part 5 of BS5400, the effective slab width ratios are defined in three Tables, which cover simply supported, cantilever, and internal spans for continuous girders. For each case, effective slab width ratios for mid-span, quarter span, and support are specified based on girder spacing to span length ratios (***s/l***). Different ratios are separately specified for uniformly distributed and concentrated load.

4.2 Canadian Specification [CSA 2000, CSA 2001]

In calculating flexural resistances and stresses in slab- on girder and box girder bridges with a concrete slab, whether girders are steel or concrete, a reduced cross-section defined by the following effective slab width criteria, i.e. Eqs. (2) and (3), shall be used. $2\bar{b}$ is the effective slab width, ***s/2*** is half girder spacing and ***l*** is the span length.

$$\frac{\bar{b}}{s/2}=1-\left\{1-\frac{l}{15s/2}\right\}^3 \qquad for \quad \frac{l}{s/2}\le 15 \tag{2}$$

$$\frac{\bar{b}}{s/2}=1 \qquad for \quad \frac{l}{s/2}>15 \tag{3}$$

4.3 Japanese Specification [JRA 1996]

In Japan, one-side effective slab width, ***λ,*** is used to calculate strength and stiffness of the girders. One-side effective slab width (λ) for uniformly distributed load and concentrate load can be computed using Eqs. (4) and (5), respectively.

$$\lambda = \begin{cases} s/2 & for \quad \frac{s/2}{l}\le 0.05 \\ \left[1.1-2\left(\frac{s/2}{l}\right)\right]s/2 & for \quad 0.05<\frac{s/2}{l}<0.3 \\ 0.15l & for \quad 0.3\le\frac{s/2}{l} \end{cases} \tag{4}$$

EU

$$\lambda = \begin{cases} s/2 & for \quad \frac{s/2}{l}\le 0.02 \\ \left[1.06-3.2\left(\frac{s/2}{l}\right)+4.5\left(\frac{s/2}{l}\right)^2\right]s/2 & for \quad 0.05<\frac{s/2}{l}<0.3 \\ 0.15l & for \quad 0.3\le\frac{s/2}{l} \end{cases} \tag{5}$$

4.4 Eurocode 4 [Eurocode 4 1992, eurocode4 1997]

In Eurocode 4, the one side effective slab width shall be taken as the distance from the centerline of the girder to the center of the outstand shear connectors plus one-eighth of the effective span length but not greater than half of the geometric slab width.

4.5 Australia Standard [AS 2327.1, 1996]

The effective width ($2\bar{b}$) shall be calculated as the sum of the distances $2\bar{b}$ /2, measured on each side of the center-line of the steel beam, where $2\bar{b}$ /2 are in each case the smallest of:

a) ***L/8***, where ***L*** is the span of the beam.
b) In the case of a concrete slab with a free edge (i.e. an edge beam situation). Either the perpendicular distance to the edge measured from the center-line of the beam, or 6 times the overall depth (h_c) of the concrete slab plus half the width of the steel beam flange (b_f).
c) In the case of a concrete slab which spans between two steel beams (i.e. either an edge beam or internal beam situation), either half the center-to-center distance between the steel beams or 8 times the overall depth (h_c) of the concrete slab plus half the width of the steel beam flange (b_f).

It must be noted that the Australian code takes into account the slab thickness in the effective slab width computations.

5. ANSYS FINITE ELEMENT MODEL

ANSYS 11.0 is a comprehensive general-purpose finite element computer program. It is capable of performing static and dynamic analysis. It is a very powerful and impressive engineering tool that may be used to solve a variety of problems.

5.1 Finite Element Model

A three-dimensional eight-node solid element (SOLID65) is used to model the concrete slab, while the steel reinforcement bar is modeled by a spar element (LINK8). The steel beam is modeled by a four-node shell element (SHELL143). A spar element (LINK8) is used to model shear connector to resist uplift; while the dowel action of shear connector is modeled by combine element (COMBIN39), in the modeling of interface between two surfaces a contact element (CONTA174) and target element (TARGE170) is used, as shown in **Fig. 6,** and the geometry of these elements is shown **Fig. 5.**

6. FINITE ELEMENT VERIFICATIONS

The verification of the finite element modeling described above can be accomplished and comparing the results generated by the finite element analysis program (ANSYS V.11) to those obtained from the experimental test. In this paper, yam and Chapman simply composite steel-concrete beam **[Yam and Chapman, 1968]** is used to verify the accuracy and performance of the finite element models used in this study.

The simply supported composite beam, tested by yam and Chapman, is one in a series of tested beams. The beam span was 5486 mm and subjected to a concentrated load at the midspan. In the present study the chosen specimen is designated as beam (E 11). The dimensions and reinforcement details of this beam are shown in **Fig. 7.**

6.1 Finite Element Idealization and Material Properties

The three-dimensional finite element mesh for one half of the beam has been used by using ANSYS 11.0 computer program, as shown in **Fig.8**. Concrete slab is idealized by using (1792) eight node brick elements (SOLID65), and steel beam is idealized by using (364) four node shell elements (SHELL143). Reinforcement is idealized by using (510) link elements (LINK8). The interface between the concrete slab and the steel beam (sticking and friction) is idealized by (112) eight node contact elements (CONTA174) and (112) eight node target elements (TARGE170). Shear connectors are idealized by (100) link elements (LINK8) to resist uplift separation. The effect of dowel action of the shear connectors through the interface between top flange of steel beam and concrete slab is idealized by (50) combine elements (COMBIN39) to resist slip. The function used to idealize the load-slip relation is:

$$Q = 31.8(1 - e^{-4.7\gamma}) \quad (6)$$

Where Q is the load on shear connector in (kN) and γ is the slip in (mm) [Yam and Chapman, 1968].

The total number of nodes resulting from the above idealization is (2871) nodes, and the total number of element is (3040) elements.

Material properties of the Yam and Chapman composite beam are summarized in **Table 2**. In this analysis the symmetry has been used by using half span of the beam. The boundary condition of this beam is shown in **Fig. 8**. The roller support is obtained by constrained displacement in y-axis, and at mid span the symmetry condition is used, the symmetry condition is obtained by constrained displacement in z-axis (longitudinal axis) for all nodes and rotations in x-axis for shell elements. The load applied (510 kN) at midspan is distributed on a rectangular area, as shown in **Fig. 8.**

The results obtained using the nonlinear finite element analysis carried out for the beam (E 11) are presented and compared with the experimental data, as shown in Table 3. The experimental and nonlinear analytical load-deflection curves are shown in **Fig. 9.**

7. PARAMETRIC STUDY

A simply supported steel-concrete composite beam tested by Yam and Chapman (E 11) has been selected to carry out the parametric study. The parameters studied can be summarized as follows:

1) Effect of Degree of Interaction.
2) Effect of Concrete Compressive Strength (f'_c).
3) Effect of Longitudinal Reinforcement.

The effect of partial interaction on Yam and Chapman composite beam has been investigated. To get full interaction, a large value for the stiffness of the shear connectors used by Yam and Chapman experimentally has been used by multiplying the stiffness value by 10^6. While for partial interaction, the number of shear connectors used by Yam and Chapman experimentally has been reduced as a percentage from the number of studs that has been used experimentally.

In this work, the uniformly distributed Load (*UDL* kN/m^2) (on the overall slab) is investigated

The nonlinear finite element analysis for the simply supported steel-concrete composite beam tested by Yam and Chapman (E 11) gave the ultimate load (500 kN) in case of (*CL*) and (190.5 kN/m^2) in case of (*UDL*). The distribution of longitudinal stresses in the slab has different shapes along the slab as shown in the **Fig. 10**. The distribution of the effective slab widths and longitudinal stresses for Yam and Chapman composite steel-concrete beam (E 11) for several stages of loading is shown in **Figs. 11 and 12.**

The effect of partial interaction on the effective slab width and the stress distribution at midspan, with various degrees of interaction, at ultimate load are shown in **Figs. 13 and 14.**

The effect of the degree of interaction on the effective slab width and maximum stress at midspan for this beam at ultimate load is listed in **Tables 4 and 5,** respectively. Comparison of effective slab width with design specifications at ultimate load is shown in **Table 6.** From the obtained results, it can be seen that when the degree of interaction increases from 24% to the used the effective slab width decreases by 10.8% and the maximum slab stress decreases by 25.6%.

The effect of concrete compressive strength on the effective slab width and maximum stress at midspan for this beam at ultimate load is listed in **Tables 7 and 8,** respectively. From the obtained results, it is seen that when the concrete compressive strength increases from (21 MPa) to (30 MPa), the effective slab width decreases by 24.5% **Fig. 15** and the maximum slab stress decreases by 28.5%, **Fig. 16**.

The effect of longitudinal reinforcement on the effective slab width and maximum stress at midspan for this beam at ultimate load is listed in **Tables 9 and 10,** respectively. From the obtained results, it is seen that when the diameter of longitudinal reinforcement increases from (Ø12 mm) to (Ø25 mm), the effective slab width increases by 40.7% , **Fig. 17** and the maximum slab stress increases by 19.7% **,Fig. 18.**

8. CONCLUSIONS

1) The results indicate good estimates of failure loads compared with experimental values. The maximum difference ratio in ultimate load is about 1.9%, while the maximum difference ratio in central deflection is about 4.7% These results reveal the accuracy and efficiency of the selected elements in ANSYS 11.0 computer program in predicting the behavior and ultimate load of composite steel-concrete beams.
2) When the degree of interaction increases from 24% to the used the effective slab width decreases by 10.8% and the maximum slab stress decreases by 25.6%.

3) When the concrete compressive strength increases from (21 MPa) to (30 MPa), the effective slab width decreases by 24.5% and the maximum slab stress decreases by 28.5%.
4) When the diameter of longitudinal reinforcement increases from (Ø12 mm) to (Ø25 mm), the effective slab width increases by 40.7% and the maximum slab stress increases by 19.7%.

REFERENCES

- AASHTO LRFD Bridge Design Specifications ,2004. A*merican Association of State Highway and Transportation Officials (AASHTO), 3rd Edition*, Washington, D.C.
- ACI Committee 318M-08, 2008. Building Code Requirements for Structural Concrete, ACI 318M-08 and Commentary, American Concrete Institute, pp. 473.
- Adekola, A. O. ,1974[a]. *The Dependence of Shear Lag on Partial Interaction in Composite Beams*, International Journal of Solids Structures, Vol.10, pp. 389-400.
- Adekola, A. O. ,1974[b]. *On Shear Lag Effects in Orthotropic Composite Beams*, International Journal of Solids and Structures, Vol. 10, pp. 735-754.
- AISC ,1986. *Load and Resistance Factor Design (LRFD), Manual of Steel Construction*, 1st Edition, American Institute of Steel Construction, pp. 1124.
- Ansourian, P. ,1975. *An Application of the Method of Finite Elements to the Analysis of Composite Floor Systems,* Proceedings of Institution of Civil Engineers, Vol. 59, pp. 699-725.
- ANSYS Manual, Version 10, 2005.
- Aref, A. J., Chiewanichakorn, M., Chen, S. S., and Ahn, S. 2007.*Effective Slab Width Definition for Negative Moment Regions of Composite Bridges*, Journal of Bridge Engineering, ASCE, Vol.12, No.3, May, pp. 339-349.
- Australia standard-composite structures, part 1: Simply Supported Beam (AS 2327.1:1996). Standards Association of Australia, New South Waels.
- BSI (1985), Structural Use of Concrete, Part 1: Code of Practice for Design and Construction, Part 2: Code of Practice for Special Circumstances, BS8110, British Standard Institution, London.
- Chiewanichakorn, M., Ahn, I-S, Aref, A. J., and Chen, S. S. , 2004.*The Development of Revised Effective Slab Width Criteria for Steel-Concrete Composite Bridges*," Structures Congress, George. E. Blandford-Editor, May, pp. 22-26.
- CSA ,2001. *Commentary on CAN/CSA-S6-00, Canadian Highway Bridge Design Code*, CSA International (cited according to Chiewanichakorn et al., 2004).
- Dezi, L., Gara, F., Leoni, G., and Tarantino, A. M. , 2001.*Time-Dependent Analysis of Shear Lag Effect in Composite Beams,* Journal of Engineering Mechanics, ASCE, Vol. 127, No. 1, January, pp. 71-79.

- Effective Slab width, 1978. Section 1.2.4, Report of Committee 41A, Monograph on Planning and Design of Tall Buildings, Vol. SB, Chap. SB-9, SACE.

- Elkelish, S., and Robinson, H. ,1986. *Effective Widths of Composite Beams with Ribbed Metal Deck,*" Canadian Journal of Civil Engineering, Vol. 13, pp. 575-582.

- Eurocode 4 ,1992. *Design of Composite Steel and Concrete Structures*, Part 1.1: general rules and rules for buildings (ENV 1994-1-1: 1992), European committee for standardization (Cited According to Chiewanichakorn et. al., 2004).

- Eurocode 4 ,1997. *Design of Composite Steel and Concrete Structures*, Part 2; Composite Bridges (ENV 1994-2: 1997), European Committee for Standardization (Cited According to Chiewanichakorn et. al., 2004).

- FIP-C and CA ,1970. *International Recommendations for the Design and Construction of Concrete Structures,* Cement and Concrete Association, London, England, pp. 39-40. Foutch, D. A., and Chang, P. C. (1982) "A Shear Lag Anomaly," Journal of the Structural Engineering, Vol. 108, No. 7, pp. 1653-1658.

- Hamply, E. C., 1976. *Bridge Deck Behavior, Chapman and Hall, London* EC4P 4EE, pp. 272.

- Heins, C. P., and Fan, H. M. ,1976. *Effective Composite Beam Width at Ultimate Load*, Journal of the Structural Division, Proceedings of the American Society of Civil Engineers, Vol. 102, No. ST 11, November, pp. 2163-2179.

- JRA ,1996. *Design Specifications for Highway Bridges (Part I- In General and Part III- Steel Bridges), Japan Road Association* (in Japanese) (cited According to Chiewanichakorn et al., 2004).

- Mackey, S. M. E., and Wong, F. K. C. ,1961.*The Effective Width of a Composite Tee-Beam Flange,* The Structural Engineer, Vol. 39, No. 9, September, pp. 277-285.

- Sun, F. F., and Bursi, O. S. , 2005. *Displacement-Based and Two-Filed Mixed Variational Formulation for Composite Beams with Shear Lag*, Journal of Engineering Mechanics, ASCE, Vol.131, No. 2, February, pp. 199-210.

- Yam, L. C. P., and Chapman, J. C. ,1968. *The Inelastic Behavior of Simply Supported Composite Beams of Steel and Concrete,* Proceedings of the Institute of Civil Engineers, Vol. 41, December, pp. 651-683.

NOMENCLATURE

The following symbols are used in this paper:-

b = one-side slab width
$\bar{b}$ = one-side effective slab width
f'_c = ultimate compressive strength (Cylinder Test)
L = span length of the beam
σ_y = normal stress in the longitudinal direction
$(\sigma_y)_{max}$ = maximum normal stress in the longitudinal direction

b_f = steel beam flange width
Q = shear force in one shear connector
γ = slip at the interface
S = spacing of beams

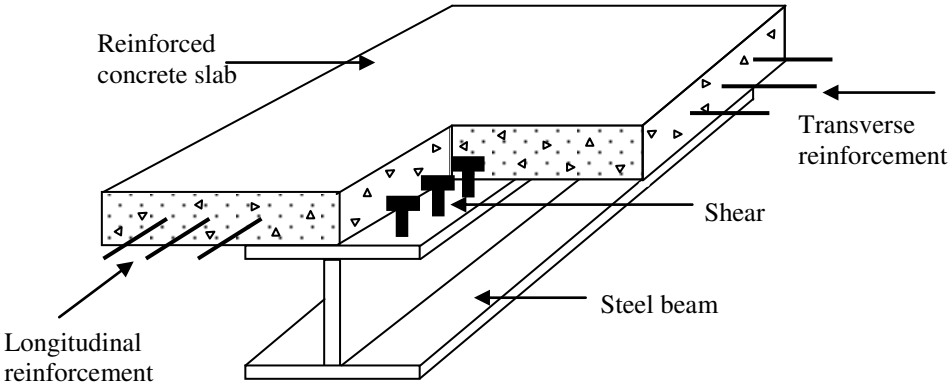

Figure 1. Composite beam components.

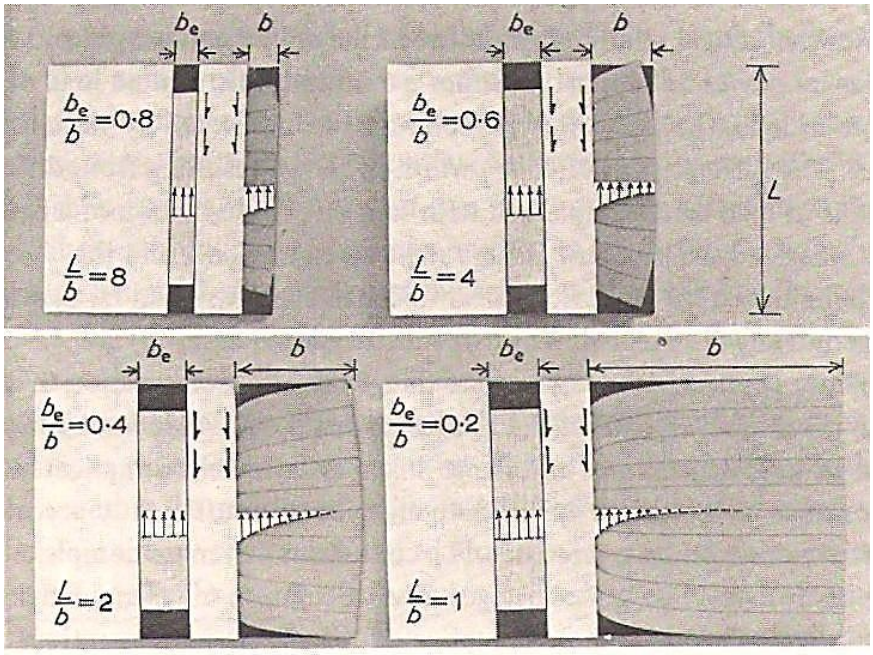

Figure 2. Shear lag distortion of flanges of various widths. [Hamply 1976].

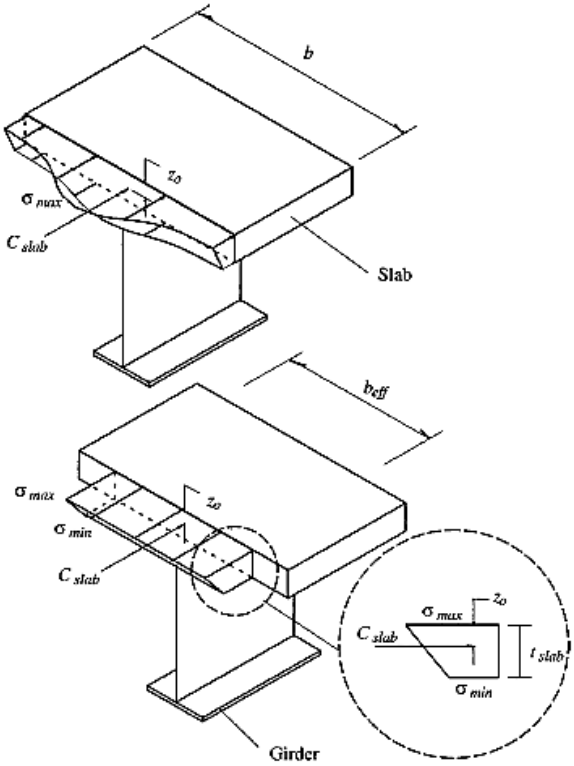

Figure 3. Effective slab width definition.
Chiewanichakorn et al., 2004[b]

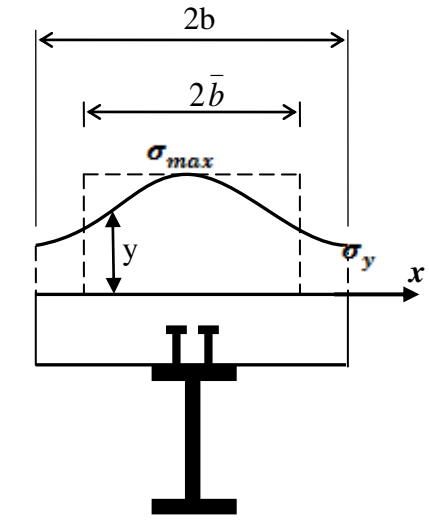

Figure 4. Effective width Definition.

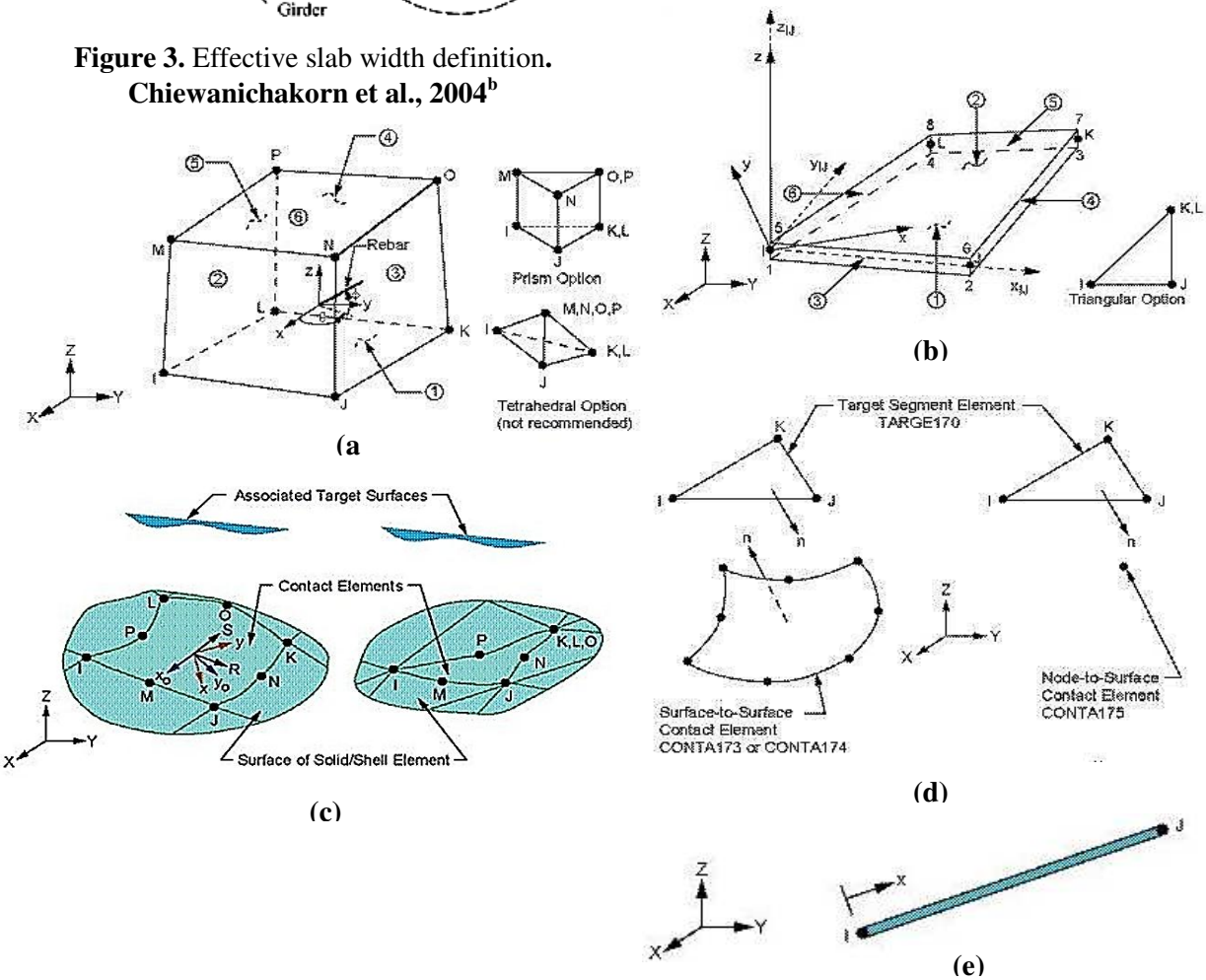

Figure 5. Elements geometry.
(a)SOLID65 (b) SHELL143 (c) CONTA174 (d) TARGE170 (e) LINK8. [ANSYS Manual 2005]

Table 1. Effective width of the slab.

Code	Formula
AASHO [AASHO, 1944]	$2\bar{b}$ **(interior beams) is the least of:** **1. L/4** **2. $12h_c$ + greater of (h_w or $b_f/2$)** **3. average (s) of adjacent beams**
AASHTO [Bowels, 1981]	$2\bar{b}$ **is least of:** **1. L/4** **2. s** **3. $12h_c$**
AASHTO-LRFD [AASHTO, 1998; AASHTO, 2004]	$2\bar{b}$ **(interior girder) is the least of:** **1. L/4** **2. $12h_c$ + greater of (h_w or $b_f/2$)** **3. average (s) of adjacent beams** $2\bar{b}$ **(exterior girder): ($2\bar{b}$ (interior girder)/2) + the least of:** **1. L/8** **2. $6h_c$ + greater of ($h_w/2$ or top $b_f/4$)** **3. overhang width**
ACI [ACI 318M-08]	$2\bar{b}$ **(interior girder) is least of:** **1. L/4** **2. s** **3.b_w + $16h_c$** $2\bar{b}$ **(exterior girder) is least of:** **1. L/12+b_w** **2. $6h_c$+b_w** **3. s/2+b_w/2**
AISC [American institute of steel construction, 1999]	$2\bar{b}$ **is the least of:** **1. L/4** **2. s** **3. $2b_e$**
BS 8110 [BSI 8110 Part 1 and Part 2, 1985]	$2\bar{b}$ **is least of:** **1. L/5+b_w** **2. s**
CEB [FIP-C and CA, 1970]	$2\bar{b}$ **= L/8 for U.D.L.** $2\bar{b}$ **= L/10 for point load.**
BS CP 117 [BSI Part 1, 1965]	$2\bar{b}$ **is least of:** **1. L/3** **2. s** **3. b_f + $12h_c$**
BS CP 117 [BSI Part 2, 1967]	**1. for s ≤ L/10:** $2\bar{b}$ **= s** **2. for s > L/10:** $(s/2\bar{b})^2 = 1+12(s/L)^2$ **but** $2\bar{b}$ **shall not be taken as less than L/10.**
Report of Committee 41A [Effective Slab Width, 1978]	$2\bar{b}$ **is the least of:** **1. L/4** **2. s** **3. $2b_e$**
Special Committee on Concrete and Reinforced Concrete [Special, 1916]	$2\bar{b}$ **is the least of:** **1. L/4** **2. 12hc**

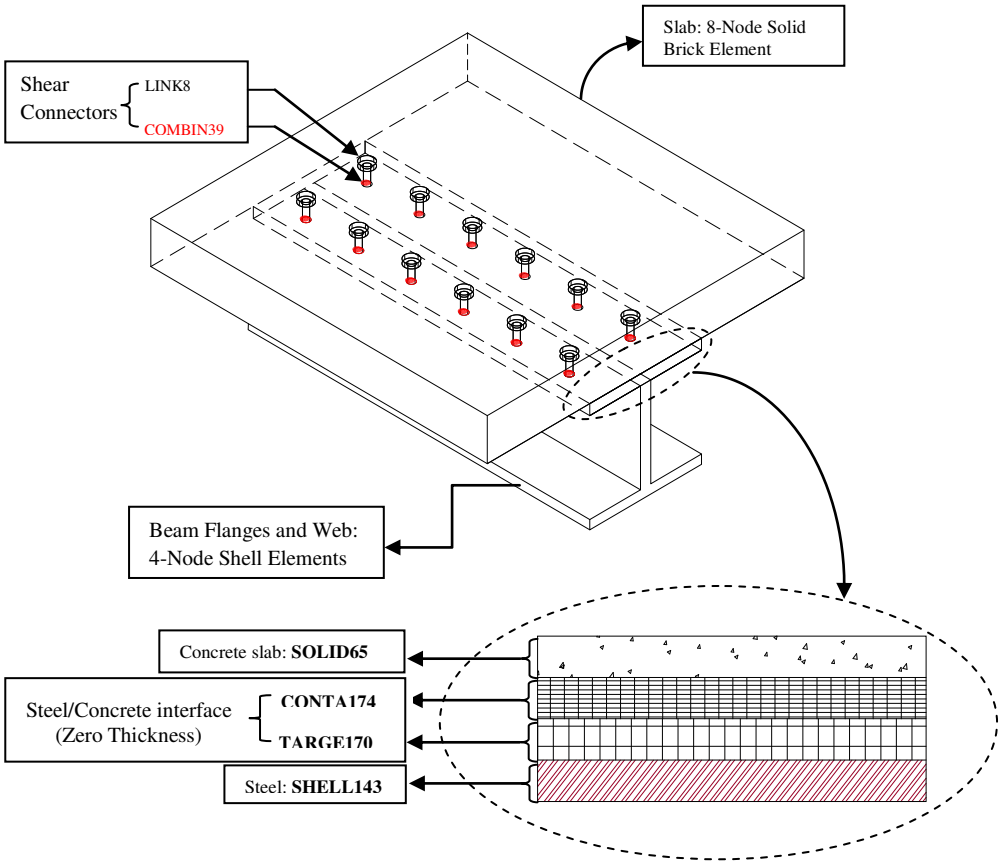

Figure 6. Schematic drawing of finite element model for composite beam.

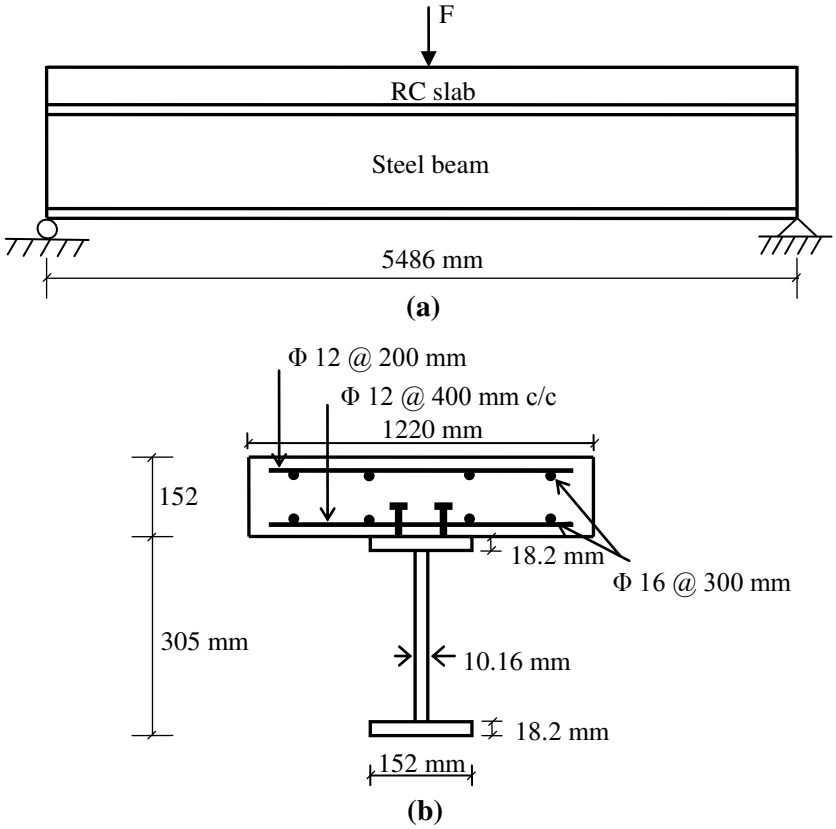

Figure 7. Yam and chapman test beam
(a) dimensions and loading arrangement of beam (e 11) (b) cross section.

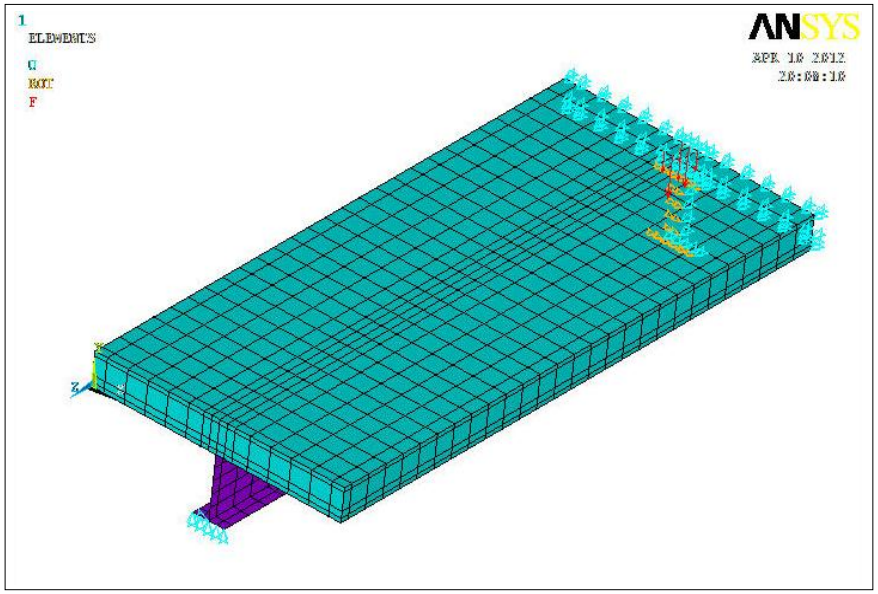

Figure 8. Three-dimensional finite element mesh for yam and chapman *composite steel-concrete beam (e 11).*

Table 2. Material properties used for yam and chapman composite steel-concrete beam (E 11).

	Symbol	Definition	Value
Concrete	f'_c	Compressive Strength (MPa)	50
	E_c	Young's Modulus (MPa)	33234
	f_r	Tensile Strength (MPa)	4.38
	υ	Poisson's Ratio	0.15*
	β_o	Shear Transfer Parameters	0.3*
	β_c		0.83*
Reinforcement	f_y	Yield Stress (MPa)	265 (Ø16)
			265 (Ø12)
	E_s	Young's Modulus (MPa)	205000
	υ	Poisson's Ratio	0.3
	E_w	Steel Hardening Parameter (MPa)	4100
Steel Beam	f_y	Yield Stress (MPa)	265
	E_s	Young's Modulus (MPa)	205000
	E_w	Steel Hardening Parameter (MPa)	4100
Shear Connector	H	Overall Height (mm)	50
	ϕ	Diameter (mm)	12
	S_{stud}	Spacing (mm)	100
	N_f	Number of Studs	100
	f_y	Yield Stress (MPa)	265
	E_s	Young's Modulus (MPa)	205000
	E_w	Steel Hardening Parameter (MPa)	4100
Interface	μ	Coefficient of Friction	0.7†

*assumed value, † [ACI 318M-08]

Note: $E_c = 4700\sqrt{f'_c}$, $E_w = 0.02\ E_s$, $f_r = 0.62\sqrt{f'_c}$

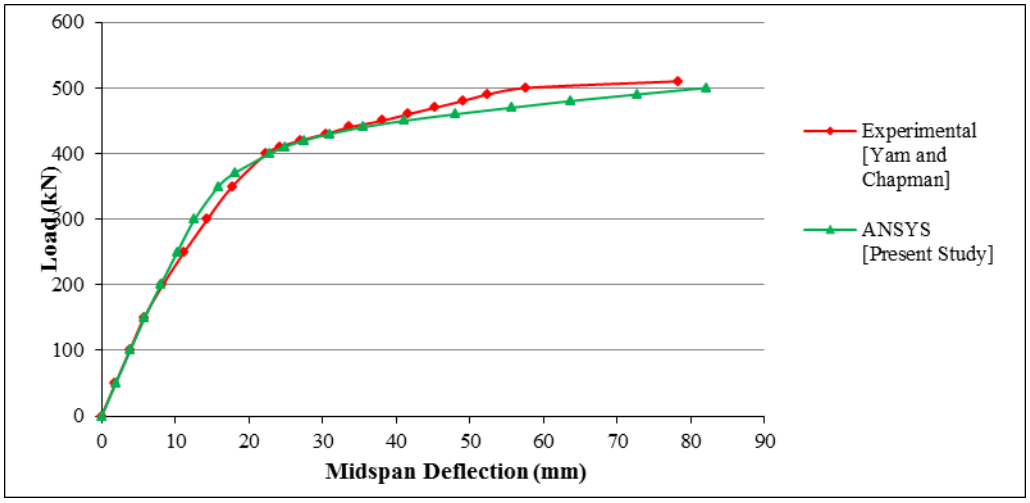

Figure.9 Experimental and nonlinear analytical load-deflection curves for yam and chapman composite beam (e 11).

Table 3. Comparison between the experimental and analytical results of yam and chapman composite beam (e 11).

Max. Central Defl. (mm)	**Experimental**	**78.4**
	Analytical	**82.1**
Ultimate Load (kN)	**Experimental**	**510**
	Analytical	**500**
$\frac{\text{Pu (Analytical)}}{\text{Pu (Experimental)}}$		**0.98**
Error in (Pu)		**-1.9%**
Failure Mode		**Concrete Crushing**

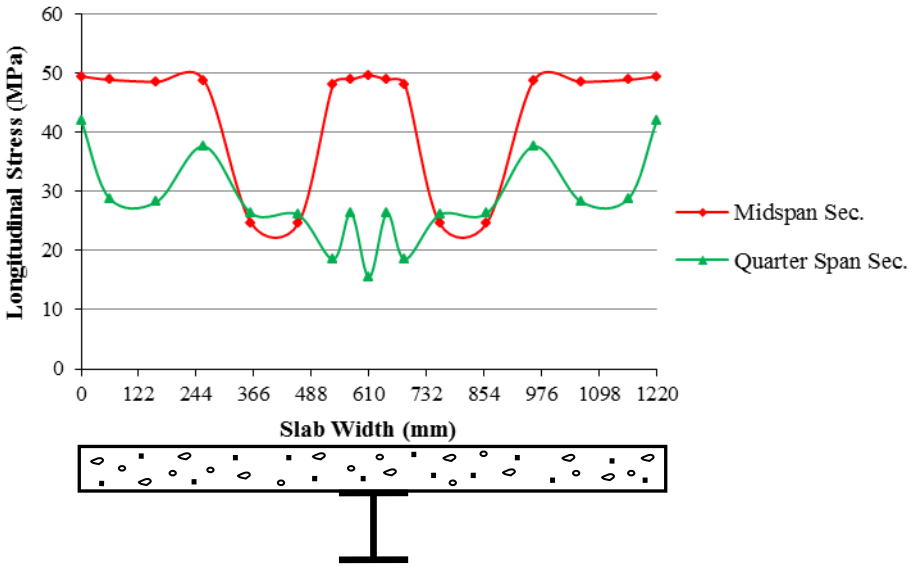

Figure 10. Slab top surface stress distribution for *udl* (190.5 kn/m^2).

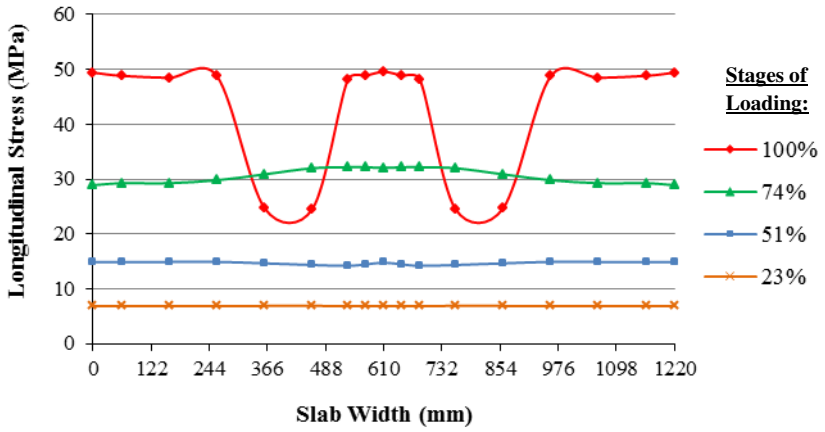

Figure 11. Slab top surface stress distribution for several stages of loading for *udl* (190.5 kn/m^2) at mid span.

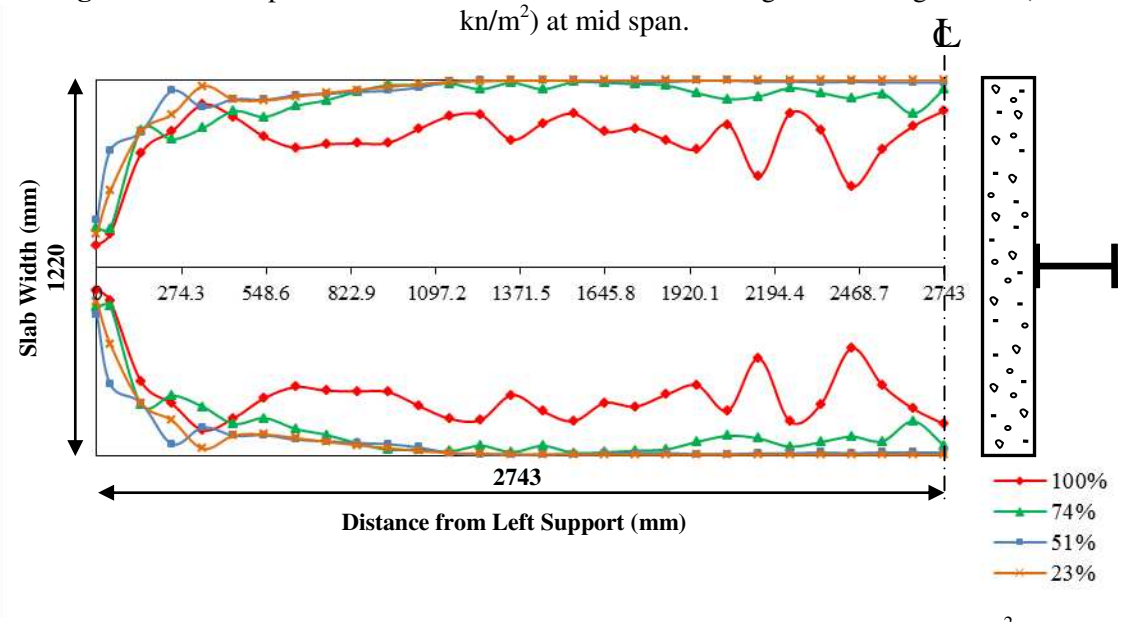

Figure 12. Effective width for several stages of loading for *udl* (190.5 kn/m^2).

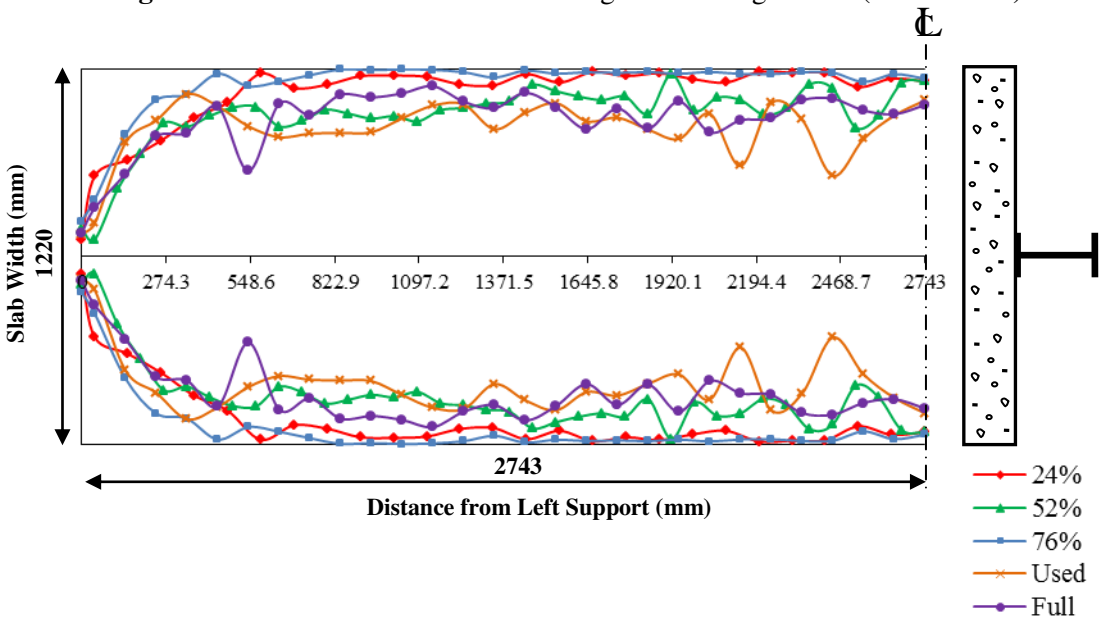

Figure 13. Effective width for various degrees of interaction at ultimate load for *UDL*.

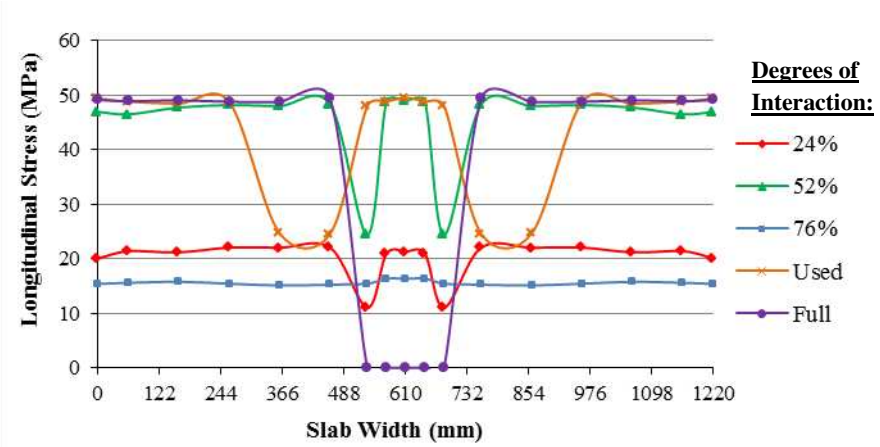

Figure 14. Effect of degree of interaction on the stress distribution in midspan section at ultimate load *UDL*.

Table 4. Effect of degree of interaction on the maximum slab stress at ultimate load in midspan for *UDL*.

Degree of Interaction (%)	Maximum Slab Stress Ratio (σ_c/σ_{ca})
24	0.753
52	0.396
76	0.431
Used	0.559
Full	0.560

Table 5. Effect of degree of interaction on the effective slab width ratio at ultimate load in midspan for *UDL*

Degree of Interaction (%)	Effective Width Ratio ($\bar{b}/b$)
24	0.934
52	0.934
76	0.948
Used	0.833
Full	0.808

Table 6. Comparison of effective slab width in midspan with design specifications at ultimate load for *UDL*

Degree of Interaction (%)	$2\bar{b}$ (mm)	ASHTTO-LRFD		ACI		AISC	BS 8110
		Exterior	Interior	Exterior	Interior		
24	1139	1144	1220	609	1220	1220	1220
52	1140	1144	1220	609	1220	1220	1220
76	1156	1144	1220	609	1220	1220	1220
Used	1017	1144	1220	609	1220	1220	1220
Full	985	1144	1220	609	1220	1220	1220

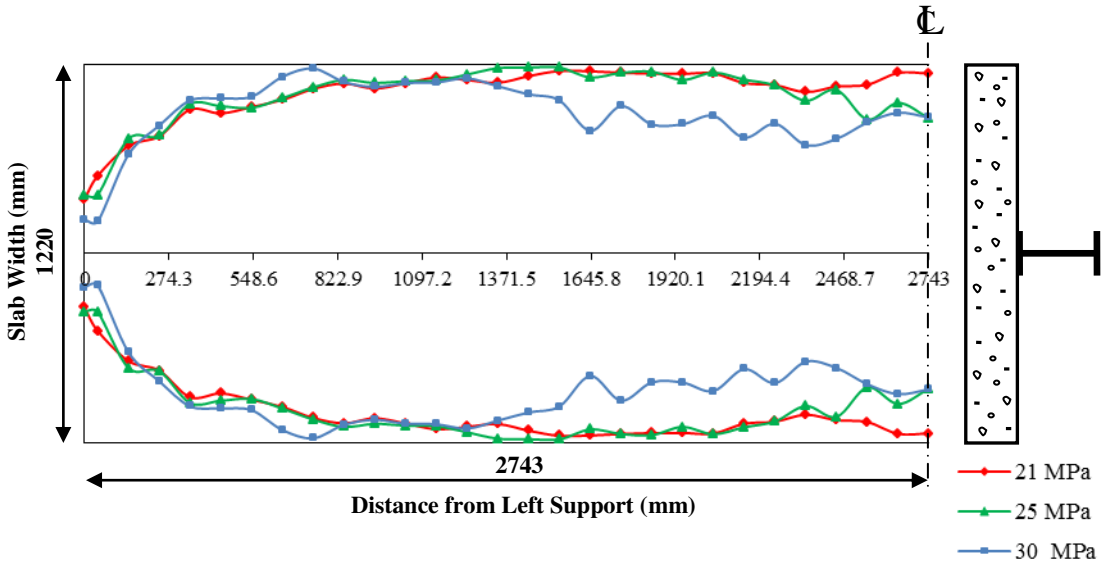

Figure 15. Effective width for various concrete strengths at ultimate load for *UDL*.

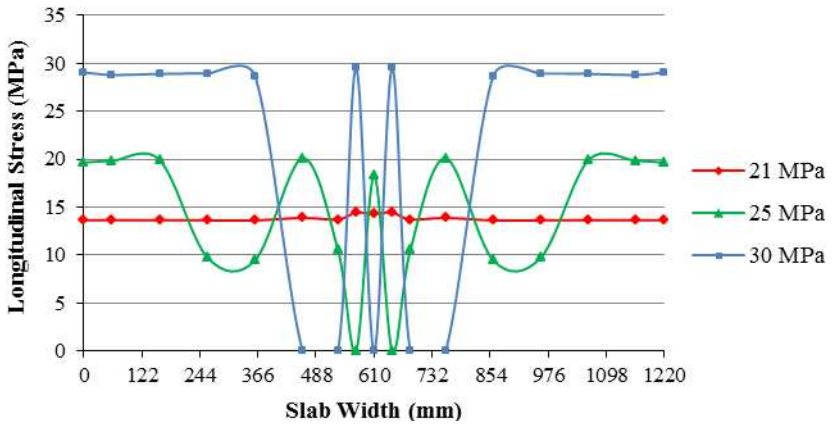

Figure 16. Effect of concrete strength on the stress distribution in midspan at ultimate load for *UDL*.

Table 7. Effect of concrete strength on the effective slab width ratio at ultimate load in midspan for *UDL*

f'_c (MPa)	Effective Width Ratio ($\bar{b}/b$)
21	0.951
25	0.714
30	0.718

Table 8. Effect of concrete strength on the maximum slab stress at ultimate load in midspan for *UDL*

f'_c (MPa)	Maximum Slab Stress Ratio (σ_c/σ_{ca})
21	0.875
25	0.837
30	

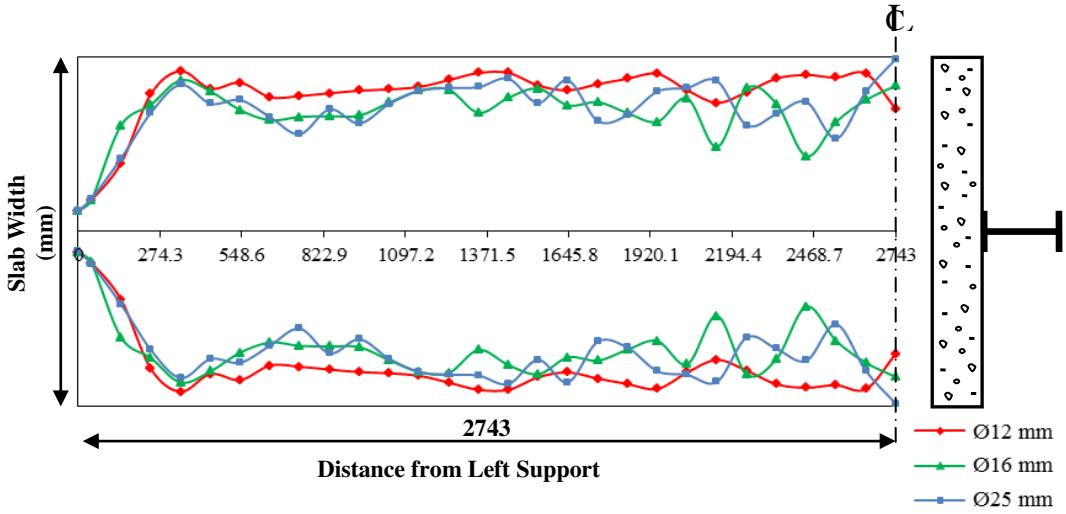

Figure 17. Effective width for various diameters of longitudinal reinforcement at ultimate load for *UDL*.

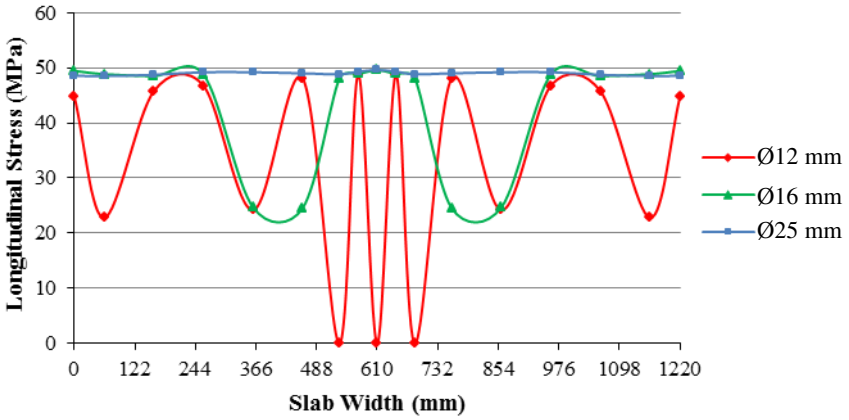

Figure 18. Effect of longitudinal reinforcement on the stress distribution in midspan at ultimate load for *UDL*.

Table 9. Effect of longitudinal reinforcement on the effective slab width ratio at ultimate load in midspan for *UDL*.

Diameter of Longitudinal Reinforcement (mm)	Effective Width Ratio ($\bar{b}/b$)
Ø12	0.701
Ø16	0.833
Ø25	0.987

Table 10. Effect of longitudinal reinforcement on the maximum slab stress at ultimate load in midspan for *UDL*

Diameter of Longitudinal Reinforcement (mm)	Maximum Slab Stress Ratio (σ_c/σ_{ca})
Ø12	0.512
Ø16	0.559
Ø25	0.613